Additively Manufactured Waveguide Hybrid Septum Coupler Optimized Using Machine Learning

Fonseca, N. J. G., Akinsolu, M. O., Rico-Fernández, J., Liu, B. and Angevain, J. -C.,

This is a paper presented at the 2024 18th European Conference on Antennas and Propagation (EuCAP), Glasgow, United Kingdom, 2024.

The published version is available at:
https://ieeexplore.ieee.org/abstract/document/10501386.

Additively Manufactured Waveguide Hybrid Septum Coupler Optimized Using Machine Learning

Nelson J. G. Fonseca*, Mobayode O. Akinsolu†, José Rico-Fernández‡, Bo Liu§, Jean-Christophe Angevain*
*European Space Agency, 2200 AG, Noordwijk, The Netherlands, {nelson.fonseca; jean.christophe.angevain}@esa.int
†Faculty of Arts, Science and Technology, Wrexham University, Wrexham, LL11 2AW U.K., m.o.akinsolu@ieee.org
‡Northern Waves AB, SE-114 28 Stockholm, Sweden, pepe.rico@northern-waves.com
§James Watt School of Engineering, University of Glasgow, Glasgow, G12 8QQ U.K., bo.liu@glasgow.ac.uk

***Abstract*—This paper describes a waveguide septum coupler design having a smooth profile well suited for additive manufacturing. The large aperture of this hybrid coupler is shaped with even-degree Legendre polynomials. Machine learning-assisted global optimization is employed to extend the operating bandwidth of the component. A design in K-band is detailed and a prototype is manufactured and tested. The experimental results confirm an improvement of 19% in operating bandwidth compared to the previously reported design in the same band while keeping all other key properties mostly unchanged, specifically the physical dimensions. The use of additive manufacturing leads to a mechanically simple and lightweight component of interest for the design of integrated microwave devices, such as beamforming networks and compact feed systems.**

***Index Terms*—Hybrid coupler, waveguide component, additive manufacturing, machine learning, communication satellite.**

I. Introduction

Directional couplers are essential microwave components with a long history going back to the 1940s [1]. They enable power-combining and power-splitting functionalities, of importance in a number of microwave sub-systems, including beamforming networks [2], phased array calibration lines [3] and circularly polarized feeds [4]. Waveguide couplers are often used in applications requiring high power operation and low insertion losses, such as satellite communications and microwave instruments [5], [6]. Well-known solutions include the Riblet coupler [7], with narrow-wall or H-plane coupling, and the branch line coupler [8], with broad-wall or E-plane coupling.

A novel patented waveguide E-plane coupler, referred to as the septum coupler, was recently proposed by some of the authors [9]. Its operating principle relies on the concept of the tandem polarizer [10], inspired from the well-known tandem coupler [11], [12]. It combines back-to-back septum polarizers providing the desired coupling level. The septum polarizer design leads to a single and large coupling aperture, which is beneficial for both manufacturing and power handling considerations.

Over recent years, there has been a growing interest for additive layer manufacturing (ALM) in the space sector [13]. This technology allows for higher integration, removing assembling screws and intermediate interfaces resulting in significant mass savings and more compact designs. A circularly polarized X-band feed including a septum coupler has already been reported using ALM [14]. Here, we explore further the degrees of freedom provided by ALM in defining the profile of the septum coupler.

Legendre polynomials have been considered for the design of septum polarizers [15]. However, the optimization process proved to be challenging as each parameter impacts the complete profile [16]. This work leverages the benefits of machine learning (ML)-assisted global optimization to obtain a new design with enhanced performance, specifically the parallel surrogate model-assisted hybrid differential evolution for antenna synthesis (PSADEA) method [19], [20]. The PSADEA is a cutting-edge ML-based technique for the efficient design of microwave devices, and it is the third instalment in the SADEA family of algorithms, which has subsequently evolved into an industry standard for the artificial intelligence (AI)-driven design of microwave devices [21]. The PSADEA does not require an initial design and any ad-hoc process, making it more robust and generic [19], [20]. Using this method, a specific K-band design is presented, which increases the operating fractional bandwidth of the previously reported prototype by 19% or 700 MHz. A prototype is manufactured using ALM and the test results are in good agreement with the predictions.

II. Waveguide Hybrid Septum Coupler With Smooth Profile

A. Design Description

A CAD view of the waveguide septum coupler discussed in this paper is provided in Fig. 1, including the definition of its main design parameters. The key differentiator with the previously reported design is its smooth profile. The hybrid septum coupler in [10] had a stepped septum profile, inspired from the stepped septum polarizer design introduced in the early 1970s [17] which is widely used nowadays in combination with conventional CNC milling manufacturing techniques. Polynomial profiles have proved to benefit the design of septum polarizers [15] and could equally improve the design of the proposed septum coupler. The smooth profiles were found to increase the operational bandwidth of septum polarizers by about 20%, while keeping other key properties mostly unchanged, specifically the physical dimensions.

In this work, we explore the use of Legendre polynomials to shape the profile of the waveguide septum coupler. The Legendre polynomials $P_n(x)$ are orthogonal polynomials of degree n which can be derived from Bonnet's recursive formula for $n > 1$ [15]:

$$(n+1)P_{n+1}(x) = (2n+1)xP_n(x) - nP_{n-1}(x), \quad (1)$$

with $P_0(x) = 1$ and $P_1(x) = x$ for $|x| \leq 1$.

While odd-degree polynomials were well suited for the design of septum polarizers [15], even-degree polynomials are preferred here as they provide the symmetry required for the septum coupler design. The first five even-degree Legendre polynomials ($n = 2k$ for $k = 0 \ldots 4$) are plotted in Fig. 2. The profile of the septum is defined with the function $S_N(x)$ for $x \in [0, L]$, obtained as the weighted sum of the first $N+1$ even-degree Legendre polynomials scaled such that the coupling aperture has a length equal to L and a maximum height equal to the broadwall dimension of the waveguides, a, for $x = 0$ and $x = L$, such that

$$S_N(x) = \frac{a}{\sum_{k=0}^{N} c_{2k}} \left(\sum_{k=0}^{N} c_{2k} P_{2k} \left(\frac{2x}{L} - 1 \right) \right), \quad (2)$$

where c_{2k}, for $k = 0 \ldots N$, are the $N+1$ weighting coefficients to be optimized.

The average lower height of the aperture is set by the coefficient c_0 of the first polynomial P_0, controlling the offset such that $S_N(x) \in [0, a]$ for $x \in [0, L]$. Here, we choose $N = 4$, resulting in 4 independent variables defining the profile of the septum, since only relative values matter due to the normalization. The objective is to extend the operational bandwidth of the previously reported design in [10] to cover the band 17 – 22 GHz. To achieve this, the PSADEA method has been used to optimize the topological profile of the waveguide septum coupler. In PSADEA, the ML engine is a Gaussian process (GP) and the global search engine is differential evolution (DE) [19], [20]. Its optimization ability primarily stems from ensuring a harmonious work between GP-based supervised learning and enhanced DE-based global search of the design space. More details about the PSADEA method can be found in [19], [20].

For the PSADEA-driven optimization of the coupler, the coefficients in (2) and the parameters in Fig. 1 have been considered, a population size of 50 is used and all other algorithmic settings are the default settings in [19], [20]. The optimization goal is to minimize the fitness function, F, defined in (3), such that $F = 0$ when all the specifications are fully met over the targeted frequency bandwidth, namely a reflection coefficient $S_{11} \leq -23$ dB, a port-to-port isolation $S_{21} \leq -23$ dB, and an axial ratio $AR \leq 0.5$ dB.

$$F = w_1 \times max([AR - 0.5\ dB, 0]) + \ \ldots$$
$$w_2 \times \{max([S_{11} + 23\ dB, 0]) + max([S_{21} + 23\ dB, 0])\}. \quad (3)$$

The weighting coefficients in F were arbitrarily set to $w_1 = 1$ and $w_2 = 50$, allowing the optimization process to preferentially ensure that S_{11} and S_{21} specifications are firstly met, before focusing on satisfying the AR specification. After 1285 EM simulations (less than 24 hours), the PSADEA method provided the septum coupler design with parameters $a = 9.80$ mm, $b = 3.48$ mm, $b_c = 7.96$ mm, $L = 15.7$ mm, and coefficients $c_2 = 0.079$, $c_4 = 0.132$, $c_6 = 0.167$, $c_8 = 0.383$, when $c_0 = 1$. The minimum value $F = 0.04$ was achieved with a marginal non-compliance on the AR.

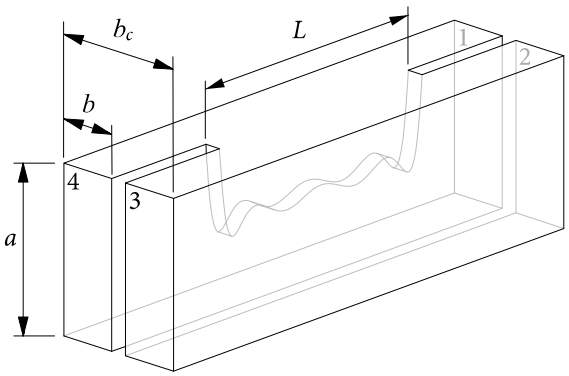

Fig. 1. Isometric CAD view of the waveguide septum coupler with port numbering and main design parameters.

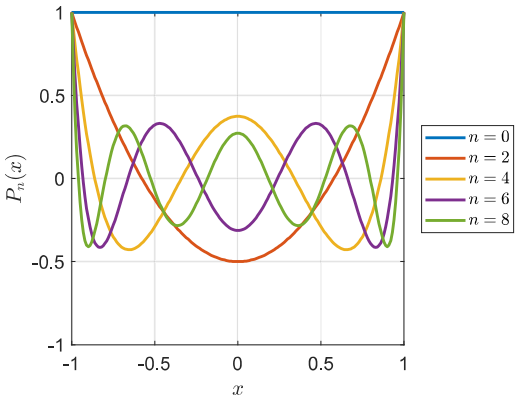

Fig. 2. First five even-degree Legendre polynomials.

B. Prototype Description

The waveguide septum coupler design described in the previous section was adapted for test purposes. Specifically, 45° bends and straight flare transitions to WR42 flanges, with cross-section dimensions $a = 10.668$ mm and $b = 4.318$ mm, are added to each port with no impact on performance. The waveguide component was manufactured using laser power bed fusion (LPBF). This ALM technique involves the sequential application and deposition of metal powder layers, each with a height ranging from 20 to 30 µm, setting the achievable tolerance [13]. The waveguide coupler was manufactured using the aluminum alloy AlSi10Mg, selected for its mechanical and electrical properties, in particular its electrical conductivity $\sigma = 1.68 \times 10^7$ S/m [18]. Moreover, a symmetrical printing orientation was deliberately selected. This decision aimed to attain a state of equilibrium and

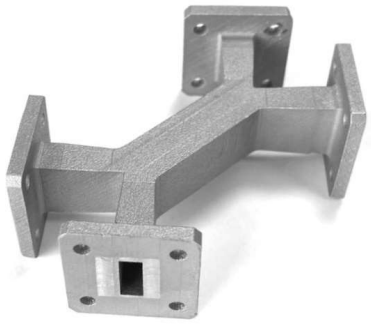

Fig. 3. Waveguide septum coupler prototype manufactured using LPBF.

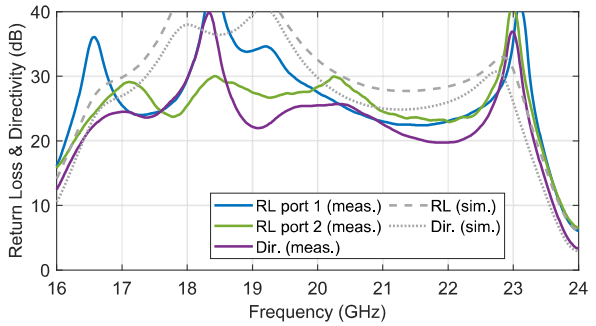

Fig. 4. Return loss and directivity of the waveguide septum coupler prototype.

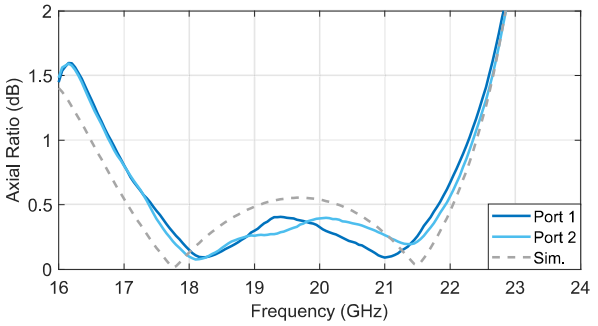

Fig. 5. Axial ratio of the waveguide septum coupler prototype.

uniform performance across all four ports, while concurrently upholding the limitations associated with overhanging angles. The prototype weights 32 g and has an estimated surface roughness of 4-6 μm, obtained with a post-processing stage using sandblasting. Finally, in order to achieve a good contact between the flanges and testing probes, a machining post-processing stage was performed in all four ports. A photograph of the prototype is provided in Fig. 3.

C. Experimental Results

The prototype was characterized using a two-port Vector Network Analyser and a WR42 calibration kit. The measured return loss and directivity (ratio of the coupling coefficient to the isolation coefficient between input ports) are compared to simulation results in Fig. 4. The measured results are slightly worse than predicted although the levels remain largely acceptable for the targeted applications, with the directivity being only marginally smaller than 20 dB at around 22 GHz. Similarly to the previously reported design [10], the operating bandwidth extends beyond the targeted range. The limiting factor is the amplitude unbalance, reported in the form of the AR in Fig. 5 to combine both the amplitude and phase variations. An AR below 0.5 dB is obtained from 17 to 22 GHz, with a small deviation around 20 GHz not exceeding 0.54 dB. In the measurements, the operating bandwidth with $AR \leq 0.5$ dB is reduced to 17.4–21.8 GHz, with small discrepancies observed between the ports 1 and 2. The results remain largely in line with expectations considering achieved manufacturing tolerances.

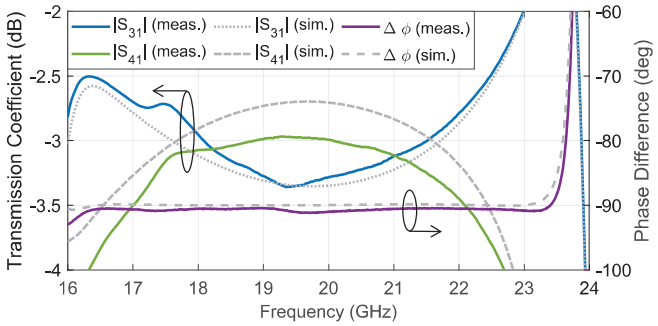

Fig. 6. Transmission coefficients and phase difference for port 1 of the waveguide septum coupler prototype.

TABLE I
COMPARISON WITH EXISTING WAVEGUIDE SEPTUM COUPLER

Reference	[10]	**This work**
Frequency bandwidth	17.2–20.9 GHz	17.4–21.8 GHz
Fractional bandwidth	19.4%	22.5%
Return loss	$>$ 23.7 dB	$>$ 22.4 dB
Directivity	$>$ 20.5 dB	$>$ 19.8 dB
Axial ratio	$<$ 0.5 dB	$<$ 0.5 dB
Insertion loss	0.11 dB	0.15 dB
Length	15.8 mm	15.7 mm
Cross-section	9.7 mm $\times$ 8.7 mm	9.8 mm $\times$ 8.0 mm
Manufacturing	CNC milling	AM

Note: the comparison is based on measured data, with the axial ratio taken as the criterion to fix the operating frequency bandwidth.

The discrepancies between measurements and predictions are further investigated reporting the transmission coefficients and phase difference for port 1 in Fig. 6. These results indicate that the phase difference is in line with predictions, with an error below 1.2° over the nominal bandwidth having no impact on the AR. The amplitude of the transmission coefficients show larger deviations, in the order of 0.3 dB, unevenly distributed between the two ports, thus impacting the AR. The insertion losses are evaluated to be quite similar to the previously reported design (0.15 dB on average over the nominal operating band, compared to 0.11 dB), indicating the discrepancies on the AR are the consequence of a slight detuning of the component due to manufacturing tolerances.

A detailed comparison of this septum coupler prototype with the one manufactured using CNC milling is provided in Table I. The measured data demonstrates an extension of

the operating bandwidth of about 19%, or 700 MHz in K-band, in line with expectations [15]. A much wider fractional bandwidth is achievable (above 30%) for applications that may tolerate larger AR values (e.g., up to 3 dB).

III. Conclusion

A waveguide hybrid septum coupler with a smooth profile was proposed. The aperture shape was defined using Legendre polynomials and the component was optimised using an AI-driven electromagnetic design method. This septum coupler design demonstrated a wider operating bandwidth compared to the stepped-septum coupler design previous reported. This smooth profile is well suited for ALM techniques and encouraging results were obtained with the prototype presented in this letter. This component is of interest for the design of integrated microwave devices, such as compact feed systems and beamforming networks.

References

[1] S. B. Cohn, and R. Levy, "History of microwave passive components with particular attention to directional couplers," *IEEE Trans. Microw. Theory Techn.*, vol. MTT-32, no. 9, pp. 1046-1054, Jul. 1984.

[2] Y. J. Guo, M. Ansari, and N. J. G. Fonseca, "Circuit type multiple beamforming networks for antenna arrays in 5G and 6G terrestrial and non-terrestrial networks," *IEEE J. Microwaves*, vol. 1, no. 3, pp. 704-722, Jul. 2021.

[3] S.-C. Chae, H.-W. Jo, J.-I. Oh, G. Kim and J.-W. Yu, "Coupler integrated microstrip patch linear phased array for self-calibration," *IEEE Antennas Wirel. Propag. Lett.*, vol. 19, no. 9, pp. 1615-1619, Sept. 2020.

[4] N. J. G. Fonseca, "Two-probe waveguide orthomode transducer with twofold rotational symmetry," *IEEE Trans. Microw. Theory Tech.*, vol. 69, no. 7, pp. 3228-3235, Jul. 2021.

[5] M. Schneider, E. Reiche, and H. Wolf, "Branch-line couplers for satellite antenna systems," in *Proc. 6^{th} German Microw. Conf.*, Darmstadt, Germany, Mar. 2011.

[6] P. Angeletti and M. Lisi, "Multimode beamforming networks for space applications," *IEEE Antennas Propag. Mag.*, vol. 56, no. 1, pp. 62-78, Feb. 2014.

[7] H. J. Riblet, "The short-slot hybrid junction," in *Proc. IRE*, vol. 40, no. 2, pp. 180–184, Feb. 1952.

[8] L. Young, "Synchronous branch guide directional couplers for low and high power applications," *IRE Trans. Microw. Theory Techn.*, vol. 10, no. 6, pp. 459–475, Nov. 1962.

[9] J.-C. Angevain and N. J. G. Fonseca, "A directional coupler and a method of manufacturing thereof," US Pat. no. 10,957,965, 23 Mar. 2021.

[10] N. J. G. Fonseca and J.-C. Angevain, "Waveguide Hybrid Septum Coupler," *IEEE Trans. Microw. Theory Techn.*, vol. 69, no. 6, pp. 3030-3036, Jun. 2021.

[11] J. P. Shelton, J. Wolfe, and R. C. Van Wagoner, "Tandem couplers and phase shifters for multi-octave bandwidths," *Microwaves*, vol. 4, pp. 14–19, Apr. 1965.

[12] H. J. Hindin and A. Rosenzweig, "3-dB couplers constructed from two tandem connected 8.34-dB asymmetric couplers," *IEEE Trans. Microw. Theory Techn.*, vol. 16, no. 2, pp. 125–126, Feb. 1968.

[13] O. A. Peverini, M. Lumia, G. Addamo, G. Virone and N. J. G. Fonseca, "How 3D-printing is changing RF front-end design for space applications," *IEEE J. Microwaves*, vol. 3, no. 2, pp. 800-814, Apr. 2023.

[14] M. Kilian, *et al.*, "Additive layer manufactured waveguide RF components," in *Proc. 49th Eur. Microw. Conf.*, pp. 790-793, Paris, France, Oct. 2019.

[15] J.-C. Angevain, N. J. G. Fonseca, "Waveguide septum polarizer shaped with Legendre polynomials," in *Proc. 11^{th} Eur. Conf. Antennas Propag. (EuCAP2017)*, Mar. 2017.

[16] N. J. G. Fonseca and J. -C. Angevain, "C-band septum polarizers with polynomial profile and accurate axial ratio characterization in back-to-back configuration," *IEEE J. Microwaves*, vol. 2, no. 4, pp. 678-689, Oct. 2022.

[17] M. H. Chen, and G. N. Tsandoulas, "A wide-band square-waveguide array polarizer", *IEEE Trans. Antennas Propag.*, vol. 21, issue 3, May 1973, pp. 389-391.

[18] S. Cassidy, A. Ian, D. Philip and G. Mikiel, "Electrical resistivity of additively manufactured AlSi10Mg for use in electric motors," *Additive Manufacturing*, May 2018, vol 21, pp. 395-403.

[19] B. Liu, M. O. Akinsolu, N. Ali, and R. Abd-Alhameed, "Efficient global optimisation of microwave antennas based on a parallel surrogate model-assisted evolutionary algorithm," *IET Microw. Antennas Propag.*. Nov. 2018, vol. 13, no. 2, pp. 149-155.

[20] M. O. Akinsolu *et al.*, "A parallel surrogate model assisted evolutionary algorithm for electromagnetic design optimization," *IEEE Trans. Emerg.*, vol. 3, no. 2, pp. 93-105, April 2019.

[21] Y. Liu *et al.*, "An efficient method for antenna design based on a self-adaptive Bayesian neural network-assisted global optimization technique," *IEEE Trans. Antennas Propag.*, vol. 70, no. 12, pp. 11375-11388, Dec. 2022.